doi:10.1006/jmbi.2000.4008 available online at http://www.idealibrary.com on IDEAL® *J. Mol. Biol.* (2000) **301**, 881–891

JMB

Time-resolved Detection of Transient Movement of Helix F in Spin-labelled Pharaonis Sensory Rhodopsin II

Ansgar-A. Wegener[1], Igor Chizhov[1], Martin Engelhard[1]* and Heinz-Jürgen Steinhoff[2]

[1]*Max-Planck-Institut für Molekulare Physiologie, Otto Hahn-Str.11, D-44227 Dortmund, Germany*

[2]*Institut für Biophysik Ruhr-Universität Bochum D-44780 Bochum Germany*

**Corresponding author*

Sensory rhodopsin II (also called phoborhodopsin) from the archaeal *Natronobacterium pharaonis* (pSRII) functions as a repellent phototaxis receptor. The excitation of the receptor by light triggers the activation of a transducer molecule (pHtrII) which has close resemblance to the cytoplasmic domain of bacterial chemotaxis receptors. In order to elucidate the first step of the signal transduction chain, the accessibility as well as static and transient mobility of cytoplasmic residues in helices F and G were analysed by electron paramagnetic resonance spectroscopy. The results indicate an outward tilting of helix F during the early steps of the photocycle which is sustained until the reformation of the initial ground state. Co-expression of pSRII with a truncated fragment of pHtrII affects the accessibility and/or the mobility of certain spin-labelled residues on helices F and G. The results suggest that these sites are located within the binding surface of the photoreceptor with its transducer.

Keywords: phoborhodopsin; bacterial signal transduction; phototaxis; site-directed spin labelling; EPR spectroscopy

Introduction

The response of Archaea and Bacteria towards external stimuli is mediated by receptor-regulated phosphorylation pathways. In the case of archaeal phototaxis, the receptors, sensory rhodopsin I and II (SRI, SRII), induce an intermolecular, probably transmembrane conformational change in their cognate transducer molecules (HtrI, HtrII) (Zhang *et al*., 1999), thereby modulating the auto-phosphorylation rate of a bound cytoplasmic histidine kinase. SRI and SRII belong to the family of visual pigment-like seven-helical membrane proteins with the two ion pumps bacteriorhodopsin (BR) and halorhodopsin as additional members. Recent progress in the structural analysis of BR and its main photo-intermediate M have revealed a movement of helix F towards the external lipid phase (Luecke *et al*., 1999a). This observation might also be of relevance for the mechanism of the signal transfer from the SR receptors to their corresponding Htr. A tilting of helix F could displace one or both of the two membrane spanning helices of the transducer protein thereby communicating the signal across the membrane.

Direct structural information on the sensory rhodopsins is not yet available. SRII from *Natronobacterium pharaonis* (pSRII) undergoes considerable alterations in the amide bond region when excited by light (Engelhard *et al*., 1996), which could be interpreted as conformational changes of the protein. In another set of experiments it could be shown that the illumination of SRI facilitates the oxidative intermolecular cross-linking of the cysteine HtrI mutant I64C (Zhang & Spudich, 1998). These experiments clearly demonstrate that HtrI exists as a dimer. Photo-activated SRI triggers conformational changes within the two HtrI molecules which influences the proximity or mobility of the two cysteine residues in position 64. The

Present addresses: H.J. Steinhoff, Max-Planck-Institut für Molekulare Physiologie, Otto Hahn-Str.11, D-44227 Dortmund, Germany.

Abbreviations used: pSRII, pharaonis sensory rhodopsin II; pHtrII, pharaonis halobacterial transducer of pSRII; t-Htr, truncated pHtrII; EPR, electron paramagnetic resonance; DM, dodecyl-maltoside; MTSSL, methanethiosulphonate spinlabel; CrOx, chromium oxalate; TM-2, second transmembrane helix; DPPH, diphenylpikrylhydrazyl; BR, bacteriorhodopsin.

E-mail address of the corresponding author: martin.engelhard@mpi-dortmund.mpg.de

0022-2836/00/040881–11 $35.00/0

interaction of receptors with their cognate transducers has been assessed by phototaxis and photocycle measurements of chimeric Htrs (Zhang *et al*., 1999). The deletion of most of the C-terminal domain of HtrI demonstrated that an N-terminal fragment of about 150 amino acid residues is sufficient to alter the photochemical properties of SRI in a similar way to the SRI/HtrI complex (Krah *et al*., 1994; Perazzona *et al*., 1996). These experiments indicated that the specificity of the SRI/HtrI interaction is confined to the two transmembrane helices and a hydrophylic stretch of 90 residues subsequent to the cytoplasmic end of TM-2.

In order to obtain more information about the structure and conformational dynamics of pSRII with and without its transducer pHtrII, site-directed spin labelling and electron paramagnetic resonance (EPR) spectroscopy is employed (for a review on site-directed spin labelling of proteins see Hubbell *et al*. (1998)). Taking recently obtained structural and EPR data from BR (Essen *et al*., 1998; Luecke *et al*., 1998; Pebay-Peyroula *et al*., 1997; Pfeiffer *et al*., 1999; Rink *et al*., 2000) into account, residues from the first and last turn of helix F (K157, S158, L159, and Y160) and helix G (F210, I211, A212, and L213), respectively (Figure 1), were mutated to cysteine and subsequently chemically modified with the methanethiosulphonate nitroxide spin label to yield the side-chain R1. To study the interaction of pSRII with its transducer, selected mutants were co-expressed with a fragment of pHtrII. The EPR spectra of these constructs enabled the elucidation of the receptor transducer interaction.

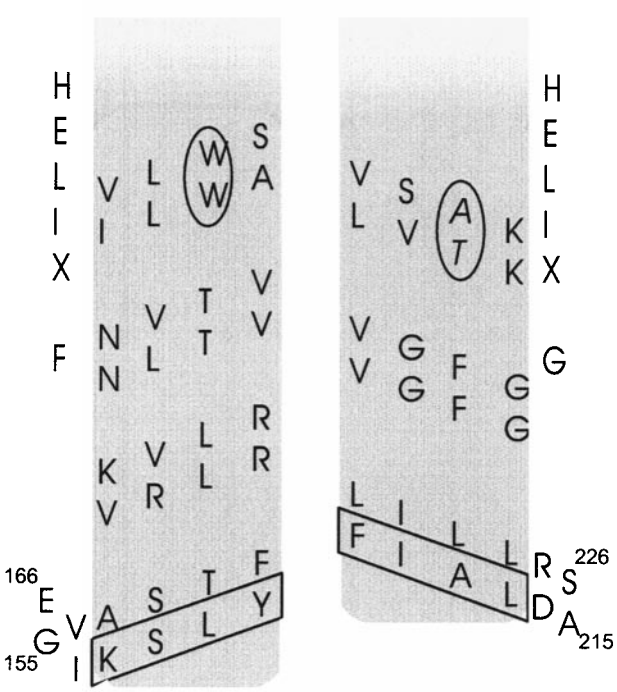

Figure 1. Sites of Cys mutations (marked by boxes). Depicted are the cytoplasmic halves of helices F and G of pSRII (lower sequence) and BR (upper sequence). Residues involved in π-bulge formation are marked by an ellipse.

Results

The mobility of nitroxide side-chains

The shape of the electron paramagnetic resonance spectra reflects the re-orientational motion of the nitroxide side-chain, which depends on the degree of interaction of the spin label with nearby groups. Strong interaction between the nitroxide and neighbouring residues of the protein results in a powder-like spectral pattern with a resolved hyperfine line in the high field region of the spectrum. This is obvious for the spectra of S158R1, L159R1, Y160R1, I211R1, A212R1 and L213R1 (Figure 2, left panel, continuous lines). The spectra are similar if not identical to those of the samples solubilized in dodecyl-maltoside (DM) (Figure 2, left panel, dotted lines), which suggests that the interactions restricting the motions are intramolecular.

The spectrum of K157R1 exhibits two distinct extremes in the low and high field regions. This may be due to an anisotropic motion of the side-chain in a certain ordering potential reflecting two conformations of the nitroxide side-chain with different sterical restrictions. The mobile component may reflect an orientation towards the exterior of the protein, whereas the immobilized component faces the protein interior. This observation would be evidence for the spin label side-chain being located close to a helix-helix contact interface. Similar spectral shapes were found for the nitroxide side-chains in bacteriorhodopsin at positions 156 and 168, which are positioned within the boundary of helices E and F (Pfeiffer *et al*., 1999).

The spectrum of F210R1 displays considerable line broadening which disappears upon solubilization in DM. Low temperature measurements (data not shown) of F210R1 reconstituted into lipids revealed dipolar as well as Heisenberg exchange interactions, indicating direct van der Waals contact of nitroxides (Miick & Millhauser, 1992). Hence, we conclude that pSRII-F210R1 forms at least dimers with the G helices in vicinity.

The accessibility of the nitroxide side-chains for paramagnetic quenchers

The motional analysis of the nitroxides was supplemented by measuring their accessibility for freely diffusing paramagnetic probe molecules (Altenbach *et al*., 1990). The collision frequency between oxygen and a spin label is low in the tightly packed interior of a protein but high in the lipid bilayer. On the other hand, collisions with water-soluble chromium oxalate (CrOx) are likely

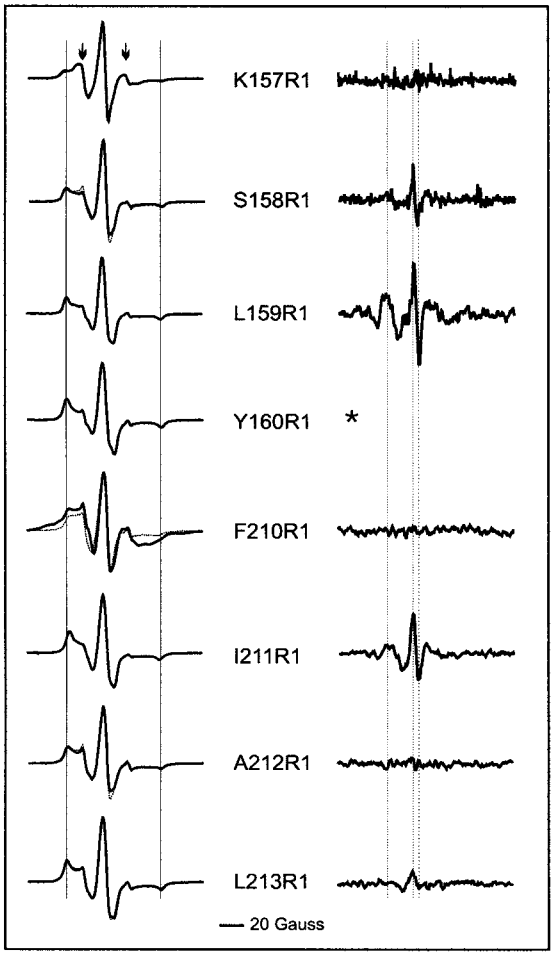

Figure 2. First derivative EPR spectra of the ground-state of spin labelled pSRII. Left panel: Spectra of samples reconstituted in PML (continuous line) and solubilized in DM (dotted line) are scaled to equal (positive) amplitude of the centre resonance. The vertical continuous lines indicate the positions of hyperfine extremes typical for strongly immobilized nitroxide labels. The arrows mark the signals of residual unbound spin label (MTSSL). Right panel: Difference spectra of spin labelled pSRII between photolysed pSRII and initial state. Dotted lines mark B-field positions used for time-resolved EPR measurements. *Y160R1 could not be reconstituted because of its low stability.

if the spin label faces the aqueous phase. As a relative measure for the collision frequency the electron longitudinal relaxation time is determined by the method of continuous wave power saturation (Altenbach *et al.*, 1989).

The data are presented in Figure 3 in terms of the dimension-less parameter Π, which is proportional to the collision frequency of the nitroxide with either oxygen or CrOx. The two-dimensional surface defined by Π_{oxygen} and Π_{CrOx} is divided into three areas, each one being characteristic for a side-chain exposed towards one of the three environments, water, lipid bilayer, or protein interior (Farahbakhsh *et al.*, 1992; Pfeiffer *et al.*, 1999). The highest collision frequency with CrOx is revealed for the side-chains attached to positions 157 and 158. These residues must be oriented towards the aqueous phase. Low values for both, Π_{CrOx} and Π_{oxygen} were found for side-chains at positions 159, 160, 211 and 213, showing that these residues have to face the protein interior. Positions 212 and 210 reveal accessibilities for oxygen typical for side-chains located at the interface between protein and lipid bilayer. The unexpectedly high accessibility of A212R1 towards oxygen might be attributed to its proximity to both the protein surface and a hydrophobic environment, as one would expect for the cytoplasmic channel. After solubilization, the value of Π_{oxygen} dramatically increases for F210R1, whereas the corresponding value for A212R1 remains unchanged. This observation further supports our conclusion derived from the analysis of the nitroxide mobility and spin-spin interaction, namely that the nitroxide at position 210 interacts with a neighbouring pSRII molecule in the native lipid bilayer. Similar dependencies on the solubilizing environment were found from an opto-acustic analysis of pSRII, which may also be interpreted as an effect of specific protein-protein interaction in the lipid bilayer (Losi *et al.*, 1999). This latter observation indicates that the dimerization is not due to the spin label but due to a general property of pSRII in lipid environment. By analogy to the orientations of corresponding amino acid side-chains of BR, a structural model of the cytoplasmic extensions of helices F and G is shown in Figure 4, which accounts for the above results.

Changes of the nitroxide mobility upon light excitation and optical spectroscopy

In order to analyse structural changes of pSRII after photo-excitation, EPR difference spectra (excited-dark state) were monitored directly during a magnetic field scan (see Materials and Methods and Steinhoff *et al.*, 1994). Considerable amplitude changes are observed in the difference spectra of L159R1 and I211R1 and in decreasing order also for S158R1 and L213R1 (Figure 2, right panel). Transient EPR signals could also be detected for K157R1 at the indicated B-field values (see below), although changes are hardly visible in the difference spectrum due to the lower signal-to-noise ratio. In all cases the spectral patterns are in line with an increased nitroxide mobility during the photocycle. In the dark state of pSRII the nitroxides of S158R1, L159R1 and I211R1 are in contact with the F-G inter-helical surface (see Figure 4). Assuming that during the photocycle helices F and G would be displaced relative to each other, the mobility of these spin label side-chains should be altered, which is indeed observed. The detected transient mobilization of these spin label side-chains including that observed for position 157 renders an outward movement of helix F likely. No mobility changes are observed for the nitroxide of F210R1, in agreement with its orientation towards

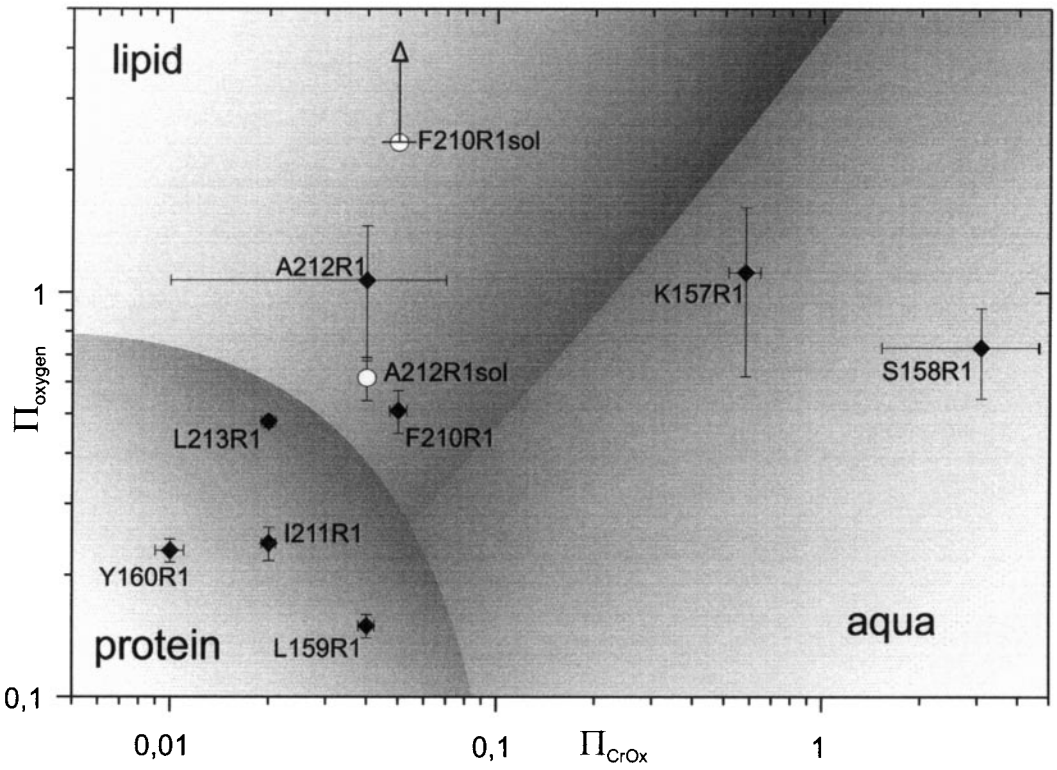

Figure 3. Accessibility diagram of lipid-reconstituted, spin-labelled pSRII (black diamonds). Π_{oxygen} allows to distinguish between a lipid or a protein environment of the nitroxide spin label. Π_{CrOx} is a measure of the accessibility for water. The borders between the three areas are empirical and drawn to guide the eye. Parameters determined for DM-solubilized A212R1 and F210R1 are also shown (open circles). For $F210R1_{sol}$ a lower limit for Π_{oxygen} had to be approximated because power saturation did not occur under the experimental conditions.

the lipid phase. At least a small movement of helix G is suggested by the difference spectrum detected for L213R1. It is interesting to note that the photocycle analysis of Y160R1 displays decreased turnover rate with a transient accumulation of the O intermediate. Similar results were obtained with the spin-labelled BR mutants F171R1 and T170R1 (Rink *et al.*, 2000). A reason for this finding could be, that the relatively larger side-chain R1 hinders helix F from returning to its original location due to sterical restrictions.

To gain more detailed information about the kinetics of the observed mobility changes the time courses of the EPR signal after photo excitation were compared with those of the optical transients (Figure 5). With the exception of Y160R1, the photocycles of the spin labelled pSRII mutants were indistinguishable from that of wild-type pSRII (Chizhov *et al.*, 1998). For all samples the rise time of the EPR signal is faster than the time resolution of the experimental set up (1 ms). Apparently, the corresponding conformational change is either faster or coincides with the formation of M (deprotonated retinal Schiff' base). The decay occurs in the time range of the recovery of the pSRII initial state (Figure 5(a) and (b); 500 nm traces) or of the reprotonation of the Schiff base (Figure 5(a) and (b); 390 nm traces). To distinguish between these two possibilities the experiments were repeated in the presence of azide, which predominantly accelerates the rate of the Schiff base reprotonation (Figure 5(c); 390 nm and 500 nm traces). It is obvious that the EPR signal follows the decay of the O-state (late photocycle intermediate) and not the reformation of the protonated Schiff base (Figure 5(c), 550 nm trace). Therefore the recovery of the initial conformation might be correlated with the re-isomerization of retinal to the all-*trans* conformation occurring during the O-decay as verified by FTIR-spectroscopy (M. Hein, F. Siebert & M.E., unpublished results). However, it should be noted that other authors concluded from FTIR and retinal extraction experiments that the O-intermediate of the SRII photocycle is characterized by an all-*trans* configuration of the retinal chromophore (Bergo *et al.*, 2000; Imamoto *et al.*, 1992).

Co-expression of pSRII with the truncated transducer

To determine the interaction of pSRII with its transducer pHtrII both membrane proteins were co-expressed in *Escherichia coli*. The construct, consisting of the open reading frame of pSRII and the entire transducer, led to serious protein aggrega-

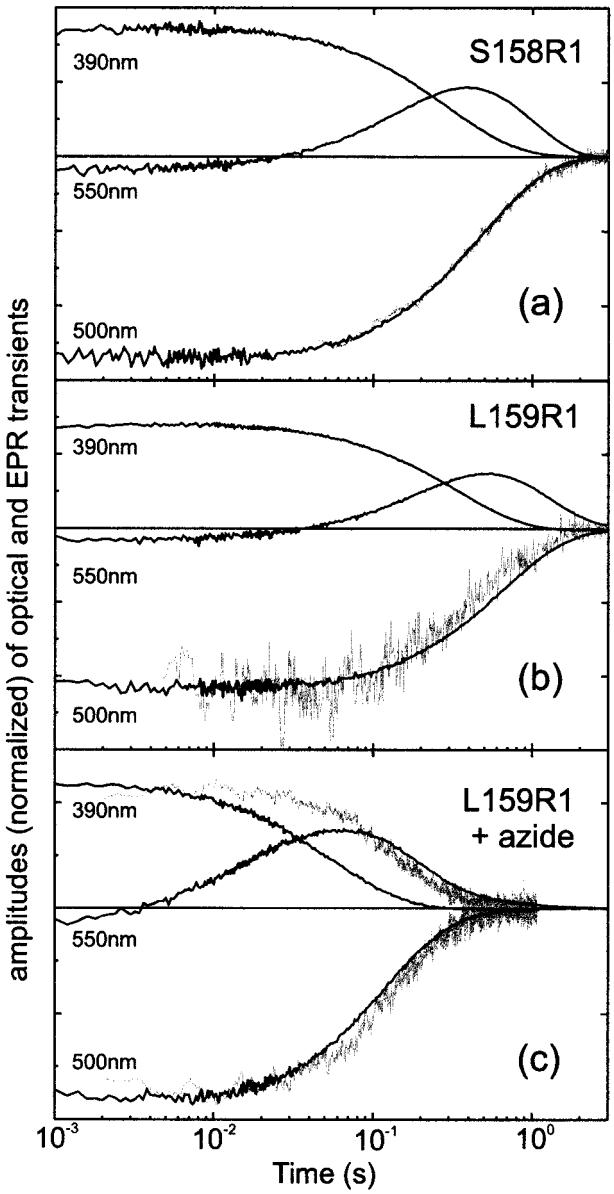

Figure 4. Transient optical absorption changes at three indicative wavelengths (500 nm → ground state; 390 nm → M; 550 nm → O) are represented by thin lines. The corresponding EPR-transient (noisy grey line) is normalised to maximal amplitude of the optical trace. (a) S158R1, (b) L159R1 both in 150 mM NaCl, 10 mM Tris (pH 8), (c) L159R1 with addition of 250 mM sodium azide at pH 7. The time resolution was 50 ms for (a) and 3 ms for (b) and (c).

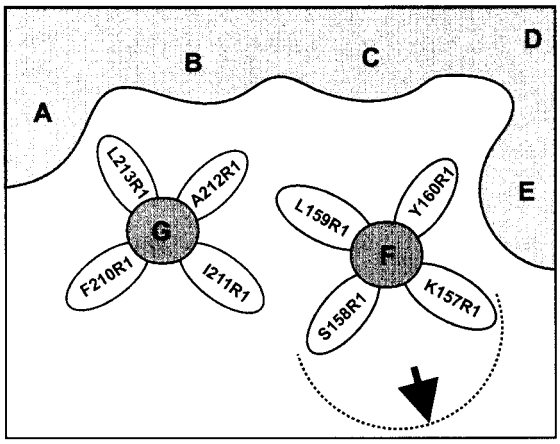

Figure 5. Arrangement of helices F and G in pSRII as deduced from the EPR data presented in this work as well as a comparison with structural data from BR (Essen *et al.*, 1998). The arrow indicates the proposed direction of the outward movement of helix F.

tion, which could hardly be purified (data not shown). Therefore, a shortened transducer was designed. Proceeding on the assumption that in HtrI and pHtrII analogous domains are involved in binding the corresponding receptors a N-terminal sequence of 159 amino acid residues was selected (Krah *et al.*, 1994; Perazzona *et al.*, 1996).

If the movement of helix F is connected to the physiological response, the outward directed residues S158R1 and F210R1 should be within or close to the interface of the transducer binding site. Therefore the constructs pSRIIS158C/t-HtrHis; pSRIIL159C/t-HtrHis; and pSRIIF210C/t-HtrHis were prepared either to monitor the transducer binding (S158, F210) or the movement of helix F (L159).

To allow for *in vivo* assembly of pSRII with t-HtrHis a plasmid was constructed with both coding sequences under the control of two independent T7-promoters. In Coomassie stained gels of total cell lysates after induction with 1 mM IPTG, a new band with an apparent molecular mass of about 18 kDa is observed which can be assigned to the truncated transducer (t-HtrHis). During the purification *via* Ni-NTA chromatography the presence of pSRII is obvious from its colour with an absorption spectrum identical in shape ($\lambda_{max} = 498$ nm) to that of wt-pSRII. In addition to t-HtrHis, pSRII-mutants become clearly visible on SDS-PAGE at an apparent molecular mass of about 22 kDa. Since the His-tag has been located at the C terminus of t-Htr the co-purification of receptor and transducer clearly indicates that both proteins do form a complex that withstands the applied conditions. The identity of the t-HtrHis was confirmed by N-terminal sequencing as well as Western-blot analysis using an antibody (rabbit) against the cytoplasmic portion of t-Htr (data not shown). The complexes were spin labelled as described above and finally purified to >90 % purity.

Effect of transducer binding on the mobility and accessibility of the nitroxide side-chains

Figure 6 represents the EPR spectra of the two mutants pSRII-S158R1 and pSRII-F210R1 in the

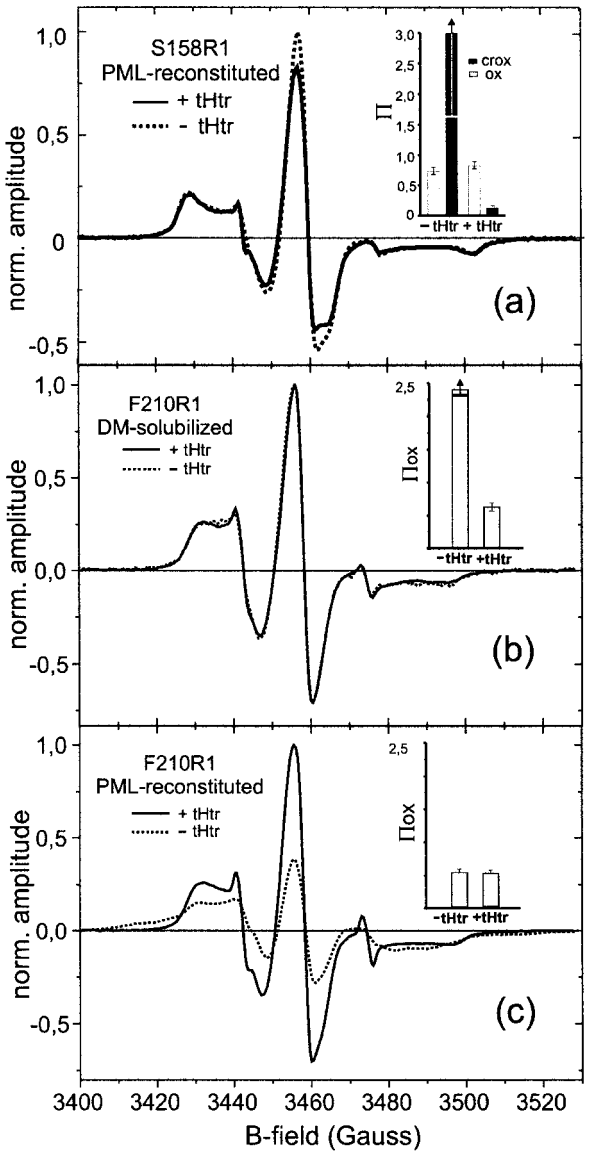

Figure 6. (a) EPR spectra of PML-reconstituted pSRIIS158R1 in the absence (dotted line) or presence (continuous line) of t-Htr normalized to constant spin number. The inset shows the dependency of accessibility parameters Π on the presence of the truncated transducer (t-Htr). (b) EPR-spectra of DM-solubilized and (c) PML-reconstituted pSRIIF210R1 in the absence (dotted line) or presence (continuous line) of t-Htr normalised to constant spin number. The insets show the dependency of the oxygen accessibility on the presence of the truncated transducer (t-Htr).

presence and absence of t-Htr. The binding of t-Htr to pSRII slightly decreases the mobility of the spin label side-chain of pSRII-S158R1 (Figure 6(a)). The accessibility of this site for CrOx is dramatically decreased (Figure 6(a), insert), indicating that it is blocked by the bound transducer. On the other hand, the values for Πox remain almost unaltered at a low level which is in line with a position of the spin-label side-chain at the protein/water boundary.

The dimerization of pSRII is hampered in reconstituted pSRII-F210R1/t-HtrHis complex as indicated by the loss of dipolar line broadening. On the other hand, the oxygen accessibility of the nitroxide at position 210 remained at the same reduced level (Figure 6(c)). These results confirm that the shortened transducer binds to pSRII in close vicinity of helices F and G. The low Πox level present even in the solubilized sample (Figure 6(b)) suggests that the interaction of pSRII with t-HtrHis is not interrupted by the detergent.

Effect of transducer binding on the light-induced changes

In the reconstituted pSRII the nitroxide of S158R1 shows a transient mobilization on light excitation (see Figure 2, right lane). In Figure 7(a) the corresponding difference spectrum is compared with the maximal amplitudes of the EPR-transients of pSRII-S158R1/t-HtrHis complex measured at three distinct B-field strengths. It is obvious that the spectral changes are oppositely directed at the respective magnetic field values. Therefore, the spin label of the transducer-bound pSRII S158R1 encounters a transient immobilization during the photocycle.

The kinetic of this process is illustrated in Figure 7(b). As can be depicted from the traces of the absorbency changes measured at 390, 500, and 550 nm in the complex, the photocycle seems to be retarded and the O-amplitude is reduced. For a detailed analysis, the data were fitted to a model in which the apparent rate constants were assigned to the irreversible steps of a unidirectional sequence of intermediates (see Müller & Plesser, 1991; Chizhov *et al.*, 1996). However, the global fit analysis revealed almost no changes of the rate constants as shown in Table 1. The assumed kinetic model allows the calculation of absolute spectra of kinetic states, which in the case of the mutant S158R1 are quite similar to those of the wild-type (Chizhov *et al.*, 1998). The states P_6 and P_7 (Figure 8), belonging to the decay times τ_6 and τ_7, represent fast quasi-equilibria between at least two archetypal chromophore states (M and O). While in P_6 the equilibrium is dominated by M, it is shifted in P_7 almost completely in favour of O. In case of transducer binding both quasi-equilibria in P_6 and P_7 are dominated by the M-state. In addition to the presence of the O-state, considerable absorption observed at 500 nm indicates the contribution of the N-state. These results can explain the apparent slower decay of the M-state which originates from the shift of the M $\Longleftrightarrow$ O partitioning in the quasi-equilibria in favour of M. It is important to note, that the variance of the photocycle is merely observed for S158R1/t-Htr but not for wild-type pSRII/t-Htr or L159R1/t-Htr.

As expected from the kinetic analysis made above, the EPR signal of S158R1/t-Htr shows a

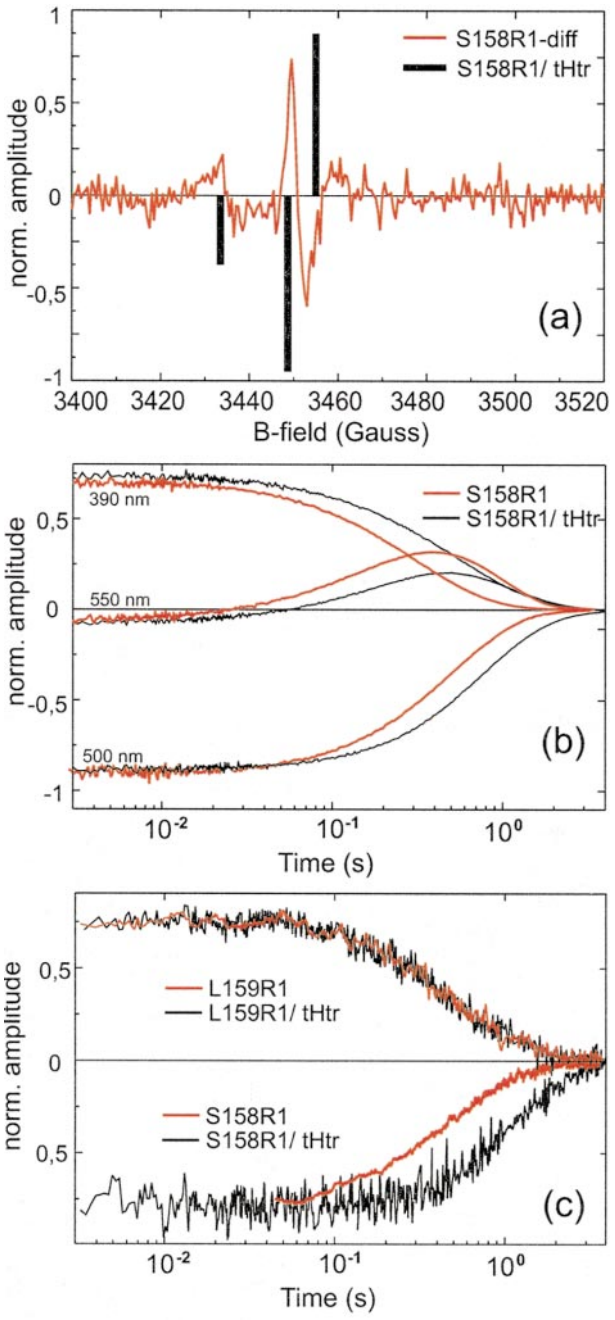

Figure 7. (a) Difference spectrum of pSRIIHisS158R1 (red line). The amplitudes of EPR-transients at different B-fields for pSRIIS158R1/t-Htr are depicted as black bars. (b) Selected optical transients of PML-reconstituted S158R1 in the absence (red) and presence (black) of t-HtrHis. All measurements were done at 25 °C in 100 mM NaCl, 10 mM Tris (pH 8). (c) EPR-transients of pSRII-mutants S158R1 and L159R1 in the absence (red) and presence (black) of t-HtrHis. The amplitudes of EPR-transients are arbitrarily normalised to allow comparison of the kinetics.

retarded decay but seemingly does not coincide with optical traces at indicative wavelengths. The calculated time constant $\tau_x \approx 1.5$ seconds for the EPR-signal decay might display the recovery of the pSRII-ground state, as it has the same order of magnitude as the corresponding time constant τ_8. It is interesting that τ_8 could not be fixed for S158R1/t-Htr in the global fit analysis of the optical data, probably due to a small optical amplitude.

In case of the mutant L159R1/t-Htr the kinetic properties of the EPR-transients are independent from the binding of the transducer fragment. Therefore the transient mobilization of the spin label at position 159 is fully maintained. This clearly points to the unimpaired outward directed movement of helix F on binding t-HtrHis.

Discussion

The results described above allow the orientation of the nitroxide side-chains bound to pSRII to be assessed in relation to their micro-environment. The immobilized spin label side-chains L159R1 and Y160R1 are orientated towards the interior of the protein. The dense atomic packing in this region prevents oxygen and CrOx reaching the nitroxide (see Figure 3). In contrast, the accessibility data of the spin label side-chains at positions K157 and S158 are evidence for their orientation towards the aqueous phase. However, the second spectral component found for K157R1 reflects a high degree of immobilization pointing to a conformation of the side-chain with considerable intra and/or intermolecular interactions. Taking the atomic data of BR (Essen *et al.*, 1998; Luecke *et al.*, 1999b) into account and assuming structural homologies, an interaction of K157R1 with helix E seems possible.

The spectra and accessibility data of the spin label side-chains I211R1, A212R1 and L213R1 in helix G reflect proximity to other nearby protein residues. By analogy to atomic coordinates of the corresponding amino acid residues in BR (I222, L223 and L224), the pSRII residues could also be oriented towards helices F, C and A. The accessibility data for F210R1 provide evidence that the spin label is oriented towards the lipid phase, whereas K157R1 and S158R1 face the aqueous phase. These results also reflect the different immersion depths of helices G and F into the lipid bilayer. Figure 4 presents a scheme of the relative orientation of helices F and G. Comparing these data with those obtained for BR, it becomes evident that helices F and G not only are similarly oriented to each other and to the other parts of the protein but have also the same boundary separating cytoplasmic residues from those immersed in the membrane.

Apparently, the structural alterations of helix F are strikingly similar for BR and pSRII. An outward movement of the cytoplasmic end of the helix has been originally proposed on the ground of electron diffraction studies of BR (Subramaniam *et al.*, 1993). In addition, recent X-ray structural analysis of BR (Luecke *et al.*, 1999a) has indicated that structural changes in the cytoplasmic part of helix G occur during the formation of M. Similar

Table 1. Rate constants of pSRII analogues and pSRII/tHtrII complexes

Protein	τ_1 (μs)	τ_2 (μs)	τ_3 (μs)	τ_4 (μs)	τ_5 (ms)	τ_6 (ms)	τ_7 (ms)	τ_8 (ms)
pSRIIHis	1.1	18	70	1800	120	250	380	1400
pSRIIHis/tHtr	1.0	13	30	1300	70	240	500	900
pSRIIS158R1	3	7	25	2000	46	190	350	1100
pSRIIS158R1/ tHtrHis	1.4	12	38	550	71	170	440	*
pSRIIL159R1	0.5	3	13	830	55	230	340	600
pSRIIL159R1/ HtrHisr	1.0	10	41	920	62	240	390	1300

Rate constants calculated by the global fit analysis of optical transients measured between 360 and 660 nm for pSRIIHis and the two mutants S158R1 and L159R1 with and without the co-purified tHtrHis. *For τ_8 of pSRIIS158R1/tHtrHis see the text.

results were obtained by Rink *et al*. (2000), who observed transient immobilization of residues in the interface of helices F and G. In contrast, the analogous residues in pSRII experience a mobilisation during the photocycle. If one takes the results of L213R1 into account, helix G undergoes only minor changes which might be directed towards helix F. The differences between pSRII and BR might be explained by the structural diversities in this region as will be described below.

The π-bulge found in BR at position Ala215 enables a hydrogen bond connection Ala215O-W501-Trp182N$^{\varepsilon}$ between helices F and G. The side-chain of Trp182 is located above the kink-region of the helix F and experiences a tilt upon retinal isomerisation. Thereby it is supposed to trigger conformational changes in helix F as it might function as a lever arm. An extensive database sequence alignment of various rhodopsins showed that Ala215(BR) is strongly conserved with the sole exception of the three known SRII-proteins bearing the more bulky threonine and serine at this position (see Figure 1). This might hinder the formation of the π-bulge in helix G. Therefore the helical movements of F and G may be disconnected, which accounts for the results described here.

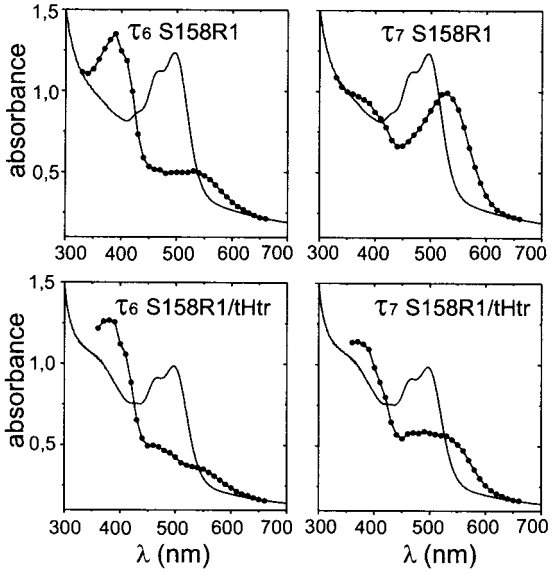

Figure 8. Absolute spectra (—●—) of kinetic states P6 and P7 derived from the difference spectra of these intermediates calculated from global fit procedure on the full wavelength scan of S158R1His and S158R1/t-HtrHis. For reasons of comparison the ground spectrum is shown in each panel (continuous line).

In a recently published review, Spudich (1998) proposed a model of a unified molecular mechanism for the archaebacterial ion-pumps and photoreceptors. The key step in the mechanism is the disruption of the salt bridge between helices C and G which triggers the outward tilting of helix F. In the case of pSRII this salt bridge exists between the protonated Schiff base and the negatively charged carboxyl group of Asp75. On light excitation the Schiff base proton is transferred to Asp75 (Bergo *et al*., 2000; Engelhard *et al*., 1996), thereby neutralizing both functional groups. Only in the last steps of the photocycle is the salt bridge reformed. The EPR data presented in this work constitute the first experimental evidence for the movement of the cytoplasmic side of helix F in pSRII, thus supporting the proposal of Spudich.

The movement of helix F may provide the trigger for the activation of the transducer as EPR experiments with the receptor-transducer complexes suggest. Although only an N-terminal fragment of pHtrII was used for the studies, it is nevertheless representative for the native complex. This assumption is justified, because the expression of pSRII-F86D together with t-HtrHis in oocytes inhibits the light-activated vectorial proton transfer as it has been observed for the full length transducer (G. Schmies, M.E., G. Nagel & E. Bamberg, unpublished results). Therefore, t-HtrHis serves as an adequate model system to elucidate the signal transfer from receptor to transducer.

The co-expression of the pSRII mutants S158R1 (helix F) and F210R1 (helix G) with t-HtrHis alters the accessibilities of the outwardly oriented spin label side-chains. These data suggest that helices F and G are close to or within the binding interface. The disintegration of the dimeric F210R1 mutant on transducer binding also supports the interaction of helices F and G with t-Htr. It is not clear which

of the two or whether both transmembrane helices of t-Htr are involved in binding to the receptor. Furthermore, the side-chain of S158R1 becomes immobilized during the photocycle, indicating that this site approaches transiently the transducer. This contact has an impact on the energetic barriers between chromophore states M, O and N, thereby changing their contribution to quasi-equilibria in favour of the M-state. Discrepancies between EPR and vis-absorption changes could be due to the specificity of monitors. Whereas the spin label senses local structural changes, absorbance changes detect alterations in the chromophore environment.

Taking recent proposals on the mechanism of chemotactic signal transfer into account (e.g. Ottemann *et al*., 1999) the C-terminal transmembrane helix (HTM-2) could be implicated.

The invariance of light-induced changes of the nitroxide mobility of L159R1 to binding of the transducer implies that the outward movement of helix F is not sterically hindered in the receptor-transducer complex. This is in line with the finding that the photocycle kinetics of this mutant and the wild-type do not change when bound to t-HtrHis. On the other hand, a modulation of the photocycle of the *Salinarum* SRII by its transducer HtrII has recently been described by Sasaki & Spudich (1998). Whether this discrepancy is due to the different receptors used has to be clarified.

In summary, the data presented in this work indicate an outward tilting of helix F which is correlated with the early steps of the photocycle and which is sustained in time over at least three orders of magnitude until the O-intermediate decays back to the ground state.

Co-expression with an N-terminal part of pHtrII provides first experimental evidence that the movement of helix F could be the trigger for a conformational change of the transducer transmembrane helices as a result of direct physical contact with the effector molecule.

Material and Methods

DNA manipulation

Bacterial strains

As a host for DNA manipulations *E. coli* XL1 was used. Gene expression was carried out in *E. coli* BL21 (DE3).

pSRII-cysteine mutants

Starting with the plasmid pET27bmod-pSRIIHis (Hohenfeld *et al*., 1999) cysteine-encoding mutations were introduced *via* a two-step PCR procedure according to the overlap extension method described by Ho *et al*. (1989). The final PCR products were ligated into pET27b-mod using the *Nco*I and *Hin*dIII restriction sites. Plasmid DNA of positive clones of *E. coli* XL1 transformants was sequenced (ABI-Prism BigDey terminator kit) to verify the introduced mutations.

Constructs for co-expression of pSRII with the transducer fragment

The DNA sequence coding for the N-terminal fragment (1-159), called t-Htr in this study, was amplified using as a template the sub-cloned *Kpn*I-*Sac*I portion of the pHtrII genomic sequence (Seidel *et al*., 1995). With the primer 5′-CGCGTCAATAACACCCATGGCGCTG-3′ and the reverse primer 5′-CGGCCTGTGAATTCGTGTT-GATCTC-3′ 5′-*Nco*I/3′-*Eco*RI restriction sites are introduced to facilitate the sub-cloning into pET27bmod (Klostermeier *et al*., 1998) with an additional His-tag. Due to this cloning strategy Ser2 is changed to Ala resulting in the following N and C-terminal sequences: **^{1}MALNV___INTEL^{159}**NSHHHHHHH. Finally, the 5′-*Bgl*II/3′-*Hin*dIII fragment of the resulting plasmid was excised which contains the t-HtrHis coding region as well as the upstream T7 promotor region.

For the co-expression construct the DNA of pSRII and of its mutants (F210C, L159C, S158C) were amplified by PCR as described (Hohenfeld *et al*., 1999) but with a modification of the reverse primer 5′-AACAGG-GGATCC*TTA*GTCGGCGACC-3′ now maintaining the original stop codon and introducing a downstream 3′-*Bam*HI site. The 5′-*Nco*I/3′-*Bam*HI-digested PCR-product was ligated into pET27bmod. The resulting plasmid was subsequently cleaved by digestion with *Bam*HI/*Hin*dIII and ligated with the 5′-*Bgl*II/3′-*Hin*dIII fragment (T7prom + t-HtrHis) described above.

Protein expression and spin labelling

pSRIIHis mutants as well as the complex pSRII/t-HtrHis were expressed in *E.coli* BL21(DE3) as described by Shimono *et al*. (1997) and purified as outlined by Hohenfeld *et al*. (1999) except that the buffer 300 mM NaCl, 25 mM sodium phosphate (pH 8) was used in all steps. For cell disruption and membrane isolation 2 mM EDTA was added. The spin label (1-oxyl-2,2,5,5-tetramethylpyrroline-3-methyl) methanethiosulphonate (MTSSL; TRC, Toronto) was covalently attached to the cysteine residues of the solubilized pSRII mutants by the method described by Pfeiffer *et al*. (1999). The label was mixed at a concentration of 1 mM with a freshly purified protein sample (300 mM NaCl, 25 mM sodium phosphate (pH 8 0), 1 % DM). Excess label was removed by Ni-NTA (Qiagen, Hilden) chromatography. The yield was about 90 % as determined by EPR and absorption spectroscopy. Finally, pSRII-mutants and the purified complex were reconstituted into purple membrane lipids as described by Losi *et al*. (1999) and buffer for all samples was adjusted to 150 mM NaCl, 10 mM Tris (pH 8).

EPR measurements

EPR cw-setup

EPR experiments were performed using a home-made EPR spectrometer equipped with a Bruker dielectric resonator. Spectra were recorded at 293 K with the microwave power set to 1.2 mW and B-field modulation amplitude adjusted to 1.5 G. The whole setup was controlled by a personal computer, which also performed 12 bit analogue-to-digital data acquisition at up to 20 kHz sample rate.

Power saturation

For power saturation experiments in the presence of molecular oxygen or chromium CrOx the samples were loaded into gas-permeable TPX capillaries (Jagmar Ltd., Kraków, Poland). The samples were deoxygenated or oxygenated by passing nitrogen or oxygen around the sample capillary. Saturation curves were determined from the peak-peak amplitudes of the centre line measured at seven different incident microwave power levels in the range from 0.5 to 80 mW. The saturation behaviour of the samples was parametrized by the quantity $P_{1/2}$, which is defined as the power level of the incident radiation at which the amplitude of the saturated line is half of the amplitude in the absence of saturation. Values for this parameter were calculated from a fitting procedure by the method of Altenbach *et al*. (1994). The $\Delta P_{1/2}$ values calculated from the difference in $P_{1/2}$ values in the presence and absence of the relaxing agent were divided by the peak-peak centre line width and normalized by the same quantity of a DPPH standard sample to obtain the dimensionless accessibility parameter Π.

Time-resolved EPR and flash photolysis

Light pulses generated by a xenon flash lamp (bulb supplied by ILC Technolgies) at approximately 80 J electrical pulse energy and 30 μs pulse duration were used for photo-excitation. Difference spectra between the photo-activated and the initial states were recorded during a single B-field scan by subtraction of EPR signals which were averaged within two different time intervals of equal length but different delays after the flash. The delays were set to 0 and one second, respectively, the length of both intervals was adjusted to one second. According to this detection scheme the EPR signal averaged during the first time interval consists of components corresponding to the photocycle intermediates.The EPR signal present after the recovery of the ground state is sampled during the second interval. The kinetics of the EPR signal changes were measured at fixed B-field values, where the difference spectra represent local extremes. The time courses of these transients were found to be independent from the selected B-field values. Between 256 and 10^3 EPR transients (3G modulation) were sampled at a rate of 0.125 s^{-1} with the integration time set to 1 or 10 ms. Optical measurements were performed with a laser flash photolysis setup similar to that described by Chizhov *et al*. (1996). For complete analysis of pSRII-mutants photo reaction, traces were recorded in the spectral range of 360-660 nm with steps of 10 nm at 25(±1) °C. 25 transients were averaged for each wavelength. Data treatment and evaluation was the same as described by Chizhov *et al*. (1998).

Acknowledgements

The financial support of the Deutsche Forschungsgemeinschaft (SFB 394, En 87 10/39) is gratefully acknowledged. We thank R.P. Seidel for providing the genomic clones of pSRII and pHtrII.

References

Altenbach, C., Flitsch, S. L., Khorana, H. G. & Hubbell, W. L. (1989). Structural studies on transmembrane proteins. 2. Spin labeling of bacteriorhodopsin mutants at unique cysteines. *Biochemistry,* **28**, 7806-7812.

Altenbach, C., Marti, T., Khorana, H. G. & Hubbell, W. L. (1990). Transmembrane protein structure: spin labeling of bacteriorhodopsin mutants. *Science,* **248**, 1088-1092.

Altenbach, C., Greenhalgh, D. A., Khorana, H. G. & Hubbell, W. L. (1994). A collision gradient method to determine the immersion depth of nitroxides in lipid bilayers: application to spin-labelled mutants of bacteriorhodopsin. *Proc. Natl Acad. Sci. USA,* **91**, 1667-1671.

Bergo, V., Spudich, E. N., Scott, K. L., Spudich, J. L. & Rothschild, K. J. (2000). FTIR analysis of the SII_{540} intermediate of sensory rhodopsin II: Asp73 is the Schiff base proton acceptor. *Biochemistry,* **39**, 2823-2830.

Chizhov, I., Chernavskii, D. S., Engelhard, M., Müller, K. H., Zubov, B. V. & Hess, B. (1996). Spectrally silent transitions in the bacteriorhodopsin photocycle. *Biophys. J.* **71**, 2329-2345.

Chizhov, I., Schmies, G., Seidel, R., Sydor, J. R., Lüttenberg, B. & Engelhard, M. (1998). The photophobic receptor from *Natronobacterium pharaonis*: temperature and pH dependencies of the photocycle of sensory rhodopsin II. *Biophys. J.* **75**, 999-1009.

Engelhard, M., Scharf, B. & Siebert, F. (1996). Protonation changes during the photocycle of sensory rhodopsin II from *natronobacterium pharaonis*. *FEBS Letters,* **395**, 195-198.

Essen, L. O., Siegert, R., Lehmannn, W. D. & Oesterhelt, D. (1998). Lipid patches in membrane protein oligomers: crystal structure of the bacteriorhodopsin-lipid complex. *Proc. Natl Acad. Sci. USA,* **95**, 11673-11678.

Farahbakhsh, Z. T., Altenbach, C. & Hubbell, W. L. (1992). Spin labelled cysteines as sensors for protein-lipid interaction and conformation in rhodopsin. *Photochem. Photobiol.* **56**, 1019-1033.

Ho, S. N., Hunt, H. D., Horton, R. M., Pullen, J. K. & Pease, L. R. (1989). Site-directed mutagenesis by overlap extension using the polymerase chain reaction. *Gene,* **77**, 51-59.

Hohenfeld, I. P., Wegener, A. A. & Engelhard, M. (1999). Purification of histidine tagged bacteriorhodopsin, *pharaonis* halorhodopsin and *pharaonis* sensory rhodopsin II functionally expressed in *Escherichia coli*. *FEBS Letters,* **442**, 198-202.

Hubbell, W. L., Gross, A., Langen, R. & Lietzow, M. A. (1998). Recent advances in site-directed spin labelling of proteins. *Curr. Opin. Struct. Biol.* **8**, 649-656.

Imamoto, Y., Shichida, Y., Hirayama, J., Tomioka, H., Kamo, N. & Yoshizawa, T. (1992). Chromophore configuration of *pharaonis* phoborhodopsin and its isomerization on photon absorption. *Biochemistry,* **31**, 2523-2528.

Klostermeier, D., Seidel, R. & Reinstein, J. (1998). Functional properties of the molecular chaperone DnaK from *Thermus thermophilus*. *J. Mol. Biol.* **279**, 841-853.

Krah, M., Marwan, W. & Oesterhelt, D. (1994). A cytoplasmic domain is required for the functional interaction of SRI and HtrI in archaeal signal transduction. *FEBS Letters,* **353**, 301-304.

Losi, A., Wegener, A. A., Engelhard, M., Gärtner, W. & Braslavsky, S. E. (1999). Time-resolved absorption and photothermal measurements with recombinant sensory rhodopsin II from *Natronobacterium pharaonis*. *Biophys. J.* **77**, 3277-3286.

Luecke, H., Richter, H. T. & Lanyi, J. K. (1998). Proton transfer pathways in bacteriorhodopsin at 2.3 Ångström resolution. *Science,* **280**, 1934-1937.

Luecke, H., Schobert, B., Richter, H. T., Cartailler, J. P. & Lanyi, J. K. (1999a). Structural changes in bacteriorhodopsin during ion transport at 2 angstrom resolution. *Science,* **286**, 255-261.

Luecke, H., Schobert, B., Richter, H. T., Cartailler, J. P. & Lanyi, J. K. (1999b). Structure of bacteriorhodopsin at 1.55 ångstrom resolution. *J. Mol. Biol.* **291**, 899-911.

Miick, S. M. & Millhauser, G. L. (1992). Rotational diffusion and intermolecular collisions of a spin labelled alpha-helical peptide determined by electron spin echo spectroscopy. *Biophys. J.* **63**, 917-925.

Müller, K.-H. & Plesser, Th. (1991). Variance reduction by simultaneous multi-exponential analysis of data sets from different experiments. *Eur. Biophys. J.* **19**, 231-240.

Ottemann, K. M., Xiao, W., Shin, Y. K. & Koshland, D. E. J. (1999). A piston model for transmembrane signaling of the aspartate receptor. *Science,* **285**, 1751-1754.

Pebay-Peyroula, E., Rummel, G., Rosenbusch, J. P. & Landau, E. M. (1997). X-ray structure of bacteriorhodopsin at 2.5 ångstroms from microcrystals grown in lipidic cubic phases. *Science,* **277**, 1676-1681.

Perazzona, B., Spudich, E. N. & Spudich, J. L. (1996). Deletion mapping of the sites on the htrI transducer for sensory rhodopsin I interaction. *J. Bacteriol.* **178**, 6475-6478.

Pfeiffer, M., Rink, T., Gerwert, K., Oesterhelt, D. & Steinhoff, H. J. (1999). Site-directed spin-labelling reveals the orientation of the amino acid side-chains in the E-F loop of bacteriorhodopsin. *J. Mol. Biol.* **287**, 163-171.

Rink, T., Pfeiffer, M., Oesterhelt, D., Gerwert, K. & Steinhoff, H. J. (2000). Unraveling photoexcited conformational changes of bacteriorhodopsin by time resolved electron paramagnetic resonance spectroscopy. *Biophys. J.* **78**, 1519-1530.

Sasaki, J. & Spudich, J. L. (1998). The transducer protein HtrII modulates the lifetimes of sensory rhodopsin II photointermediates. *Biophys. J.* **75**, 2435-2440.

Seidel, R., Scharf, B., Gautel, M., Kleine, K., Oesterhelt, D. & Engelhard, M. (1995). The primary structure of sensory rhodopsin II: a member of an additional retinal protein subgroup is coexpressed with its transducer, the halobacterial transducer of rhodopsin II. *Proc. Natl Acad. Sci. USA,* **92**, 3036-3040.

Shimono, K., Iwamoto, M., Sumi, M. & Kamo, N. (1997). Functional expression of pharaonis phoborhodopsin in *Escherichia coli*. *FEBS Letters,* **420**, 54-56.

Spudich, J. L. (1998). Variations on a molecular switch - transport and sensory signalling by archaeal rhodopsins. *Mol. Microbiol.* **28**, 1051-1058.

Steinhoff, H.-J., Mollaaghababa, R., Altenbach, C., Hideg, K., Krebs, M., Khorana, H. G. & Hubbell, W. L. (1994). Time-resolved detection of structural changes during the photocycle of spin-labelled bacteriorhodopsin. *Science,* **266**, 105-107.

Subramaniam, S., Gerstein, M., Oesterhelt, D. & Henderson, R. (1993). Electron diffraction analysis of structural changes in the photocycle of bacteriorhodopsin. *EMBO J.* **12**, 1-8.

Zhang, X.-N. & Spudich, J. L. (1998). HtrI is a dimer whose interface is sensitive to receptor photoactivation and His-166 replacements in sensory rhodopsin I. *J. Biol. Chem.* **273**, 19722-19728.

Zhang, X. N., Zhu, J. & Spudich, J. L. (1999). The specificity of interaction of archaeal transducers with their cognate sensory rhodopsins is determined by their transmembrane helices. *Proc. Natl Acad. Sci. USA,* **96**, 857-862.

Edited by W. Baumeister

(Received 18 April 2000; received in revised form 30 June 2000; accepted 4 July 2000)